

## Supplementary Information for

# Bi<sub>2</sub>OS<sub>2</sub>: a Direct-Gap Two-dimensional Semiconductor with High Carrier Mobility and Surface Electron States

Xiwen Zhang<sup>‡a</sup>, Bing Wang<sup>‡b</sup>, Xianghong Niu<sup>c</sup>, Yunhai Li<sup>b</sup>, Yunfei Chen<sup>d\*</sup> and  
Jinlan Wang<sup>b\*</sup>

<sup>a</sup> *School of Mechanism Engineering & School of Physics, Southeast University, Nanjing  
211189, China*

<sup>b</sup> *School of Physics, Southeast University, Nanjing 211189, China*

<sup>c</sup> *School of Science, Nanjing University of Posts and Telecommunications, Nanjing 210046,  
China*

<sup>d</sup> *School of Mechanism Engineering, Southeast University, Nanjing 211189, China*

‡ Xiwen Zhang and Bing Wang contributed equally to this work.

Corresponding Authors: \*E-mail: [jlwang@seu.edu.cn](mailto:jlwang@seu.edu.cn); [yunfeichen@seu.edu.cn](mailto:yunfeichen@seu.edu.cn)

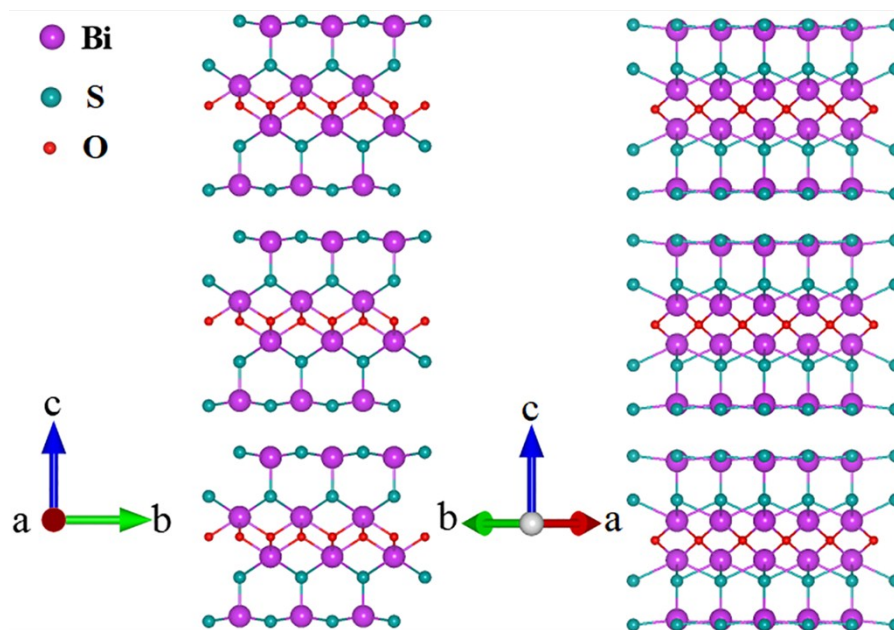


**Fig. S1** Structure of bulk  $\text{Bi}_2\text{OS}_2$  in a  $3\times 3\times 3$  supercell from different views.

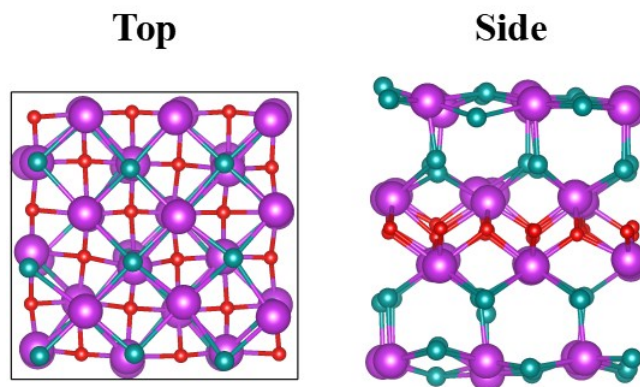


**Fig. S2** Snapshots of atomic configurations of  $\text{Bi}_2\text{OS}_2$  monolayer at temperatures of 500 K at the end of 5 ps.

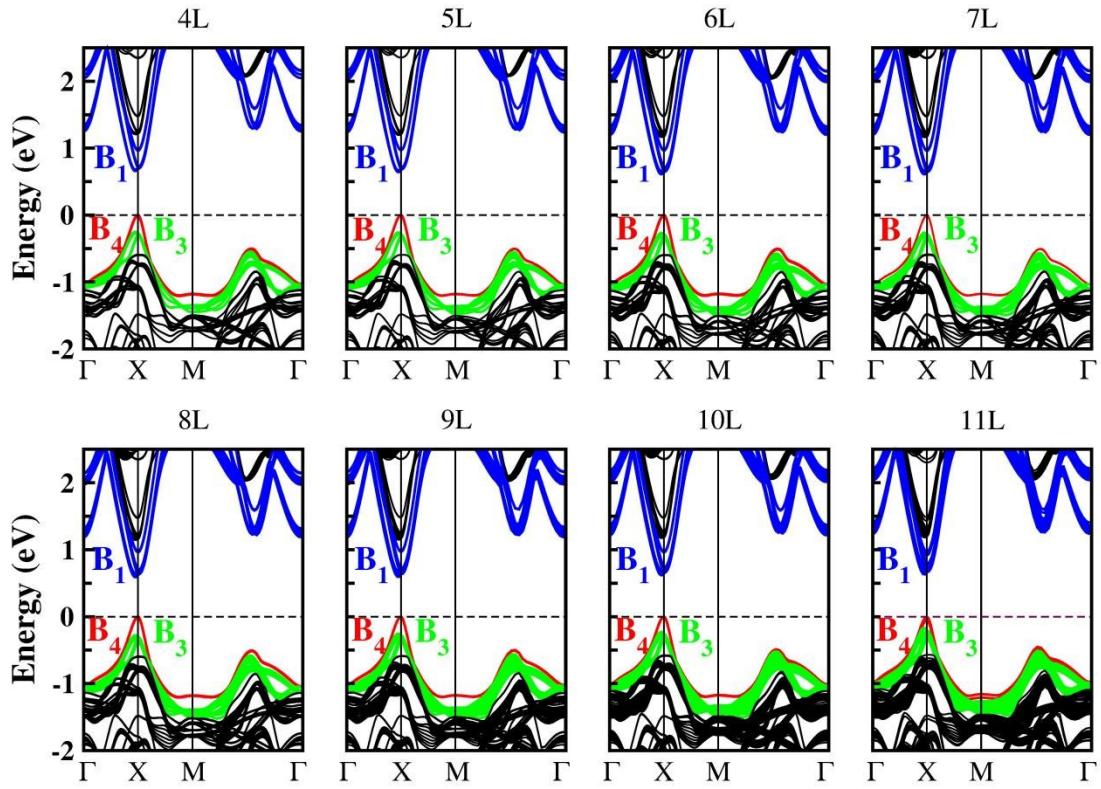


Fig. S3 Calculated band structures of 2D  $\text{Bi}_2\text{OS}_2$  from 4L to 11L. Top of the valence band is set to zero.

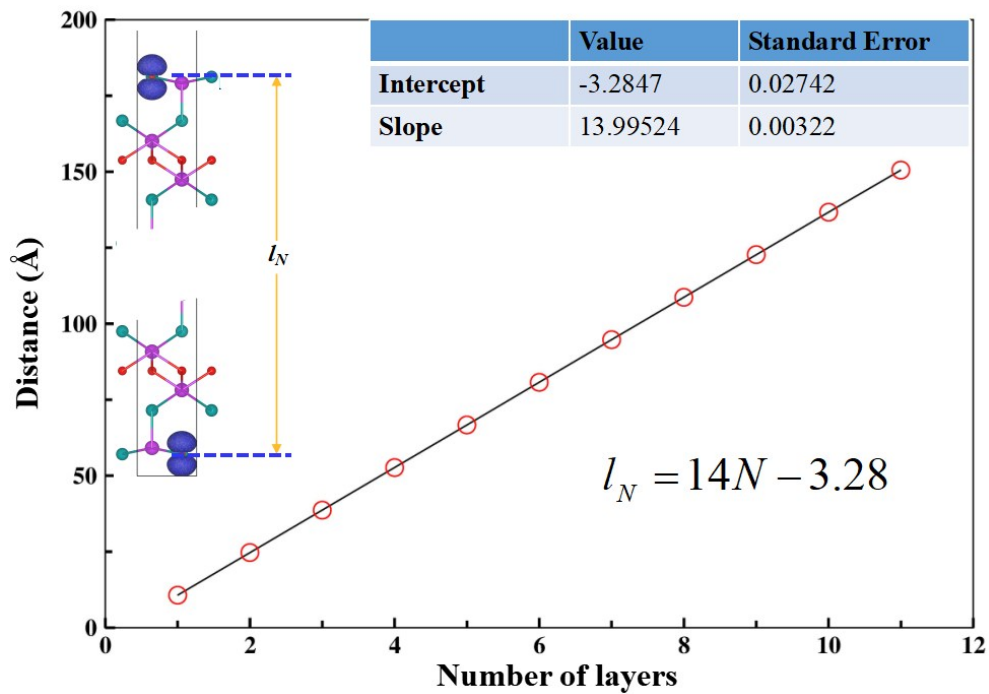
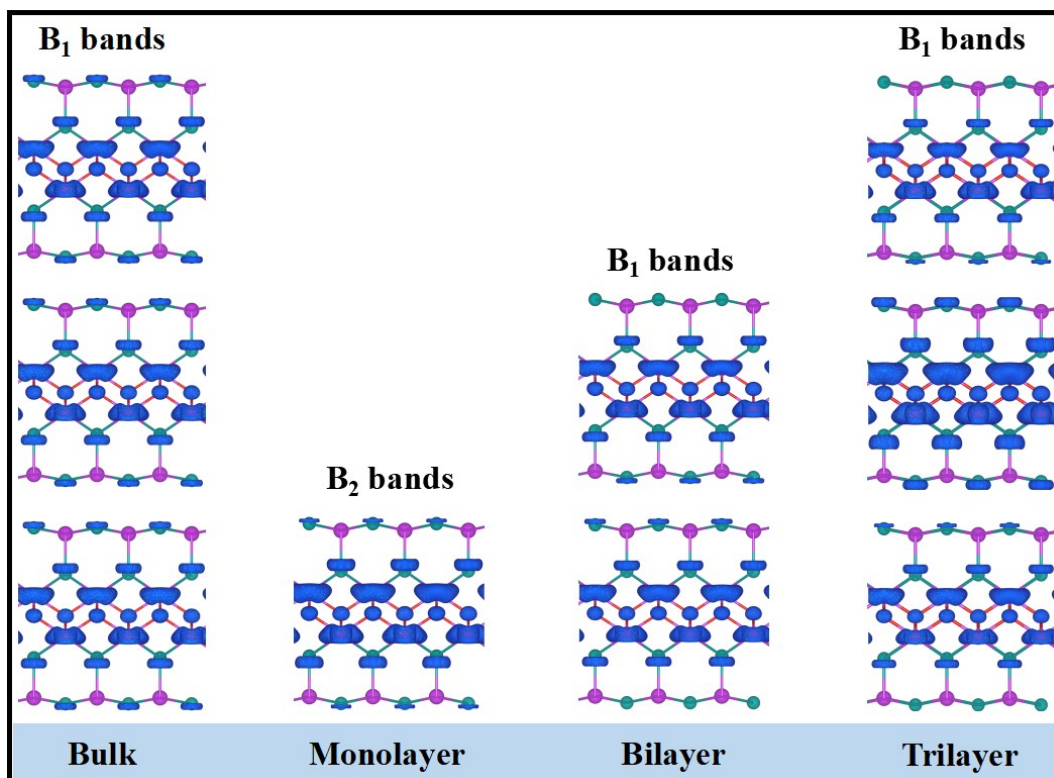
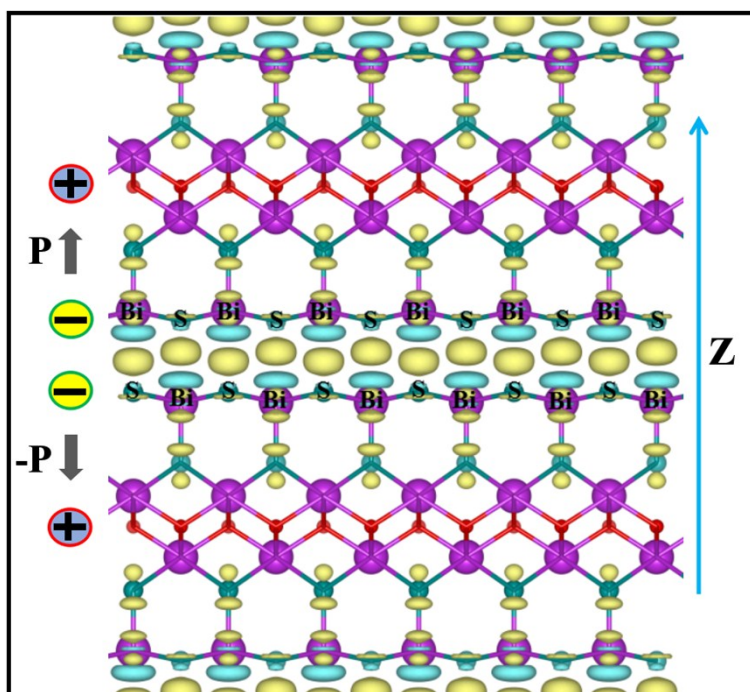


Fig. S4 The distance between the two outermost layers exhibits a linear dependence on the number of layers.



**Fig. S5** Calculated band decomposed charge density of the  $B_1$  and  $B_2$  bands (labeled in Figure 2a) with the isosurface values of  $0.01 \text{ e/bohr}^3$ .



**Fig. S6** Different charge densities for the bulk  $\text{Bi}_2\text{OS}_2$  with an isovalue of  $0.0007 \text{ e/bohr}^3$ . The cyan and yellow regions represent the charge depletion and accumulation in the space, respectively.

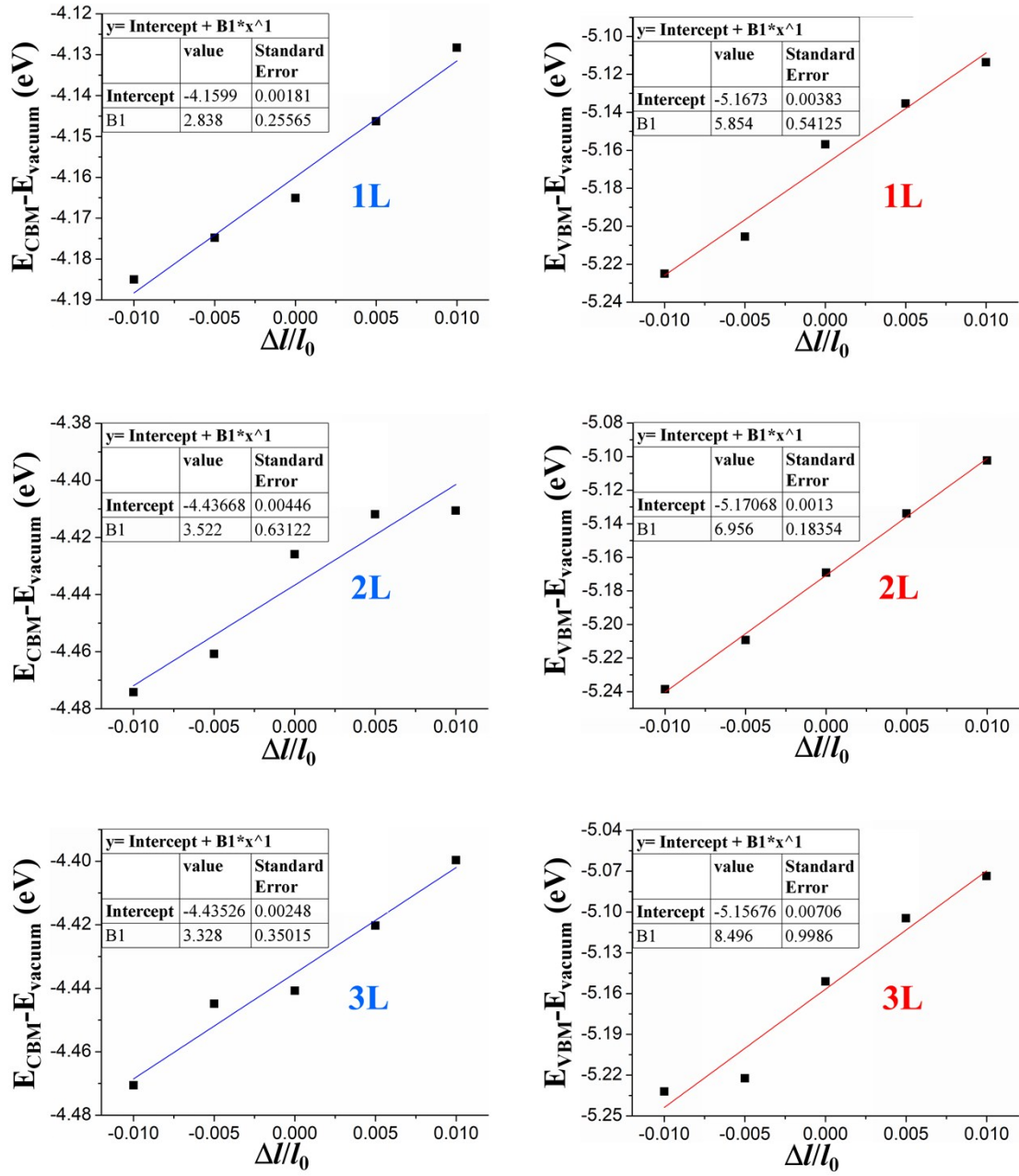


**Fig. S7** Linear fitting of deformation potential. Energy change of the CBMs and VBMs of Bi<sub>2</sub>OS<sub>2</sub> mono- and few layers with respect to the vacuum level as a function of lattice dilation.

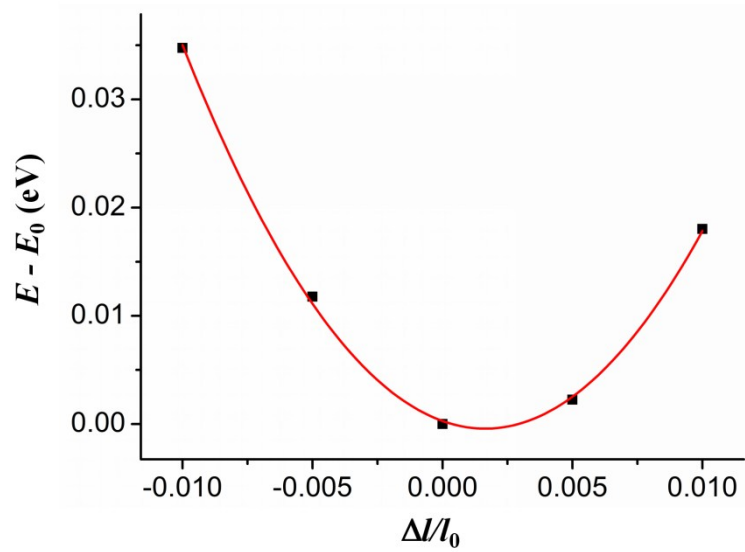
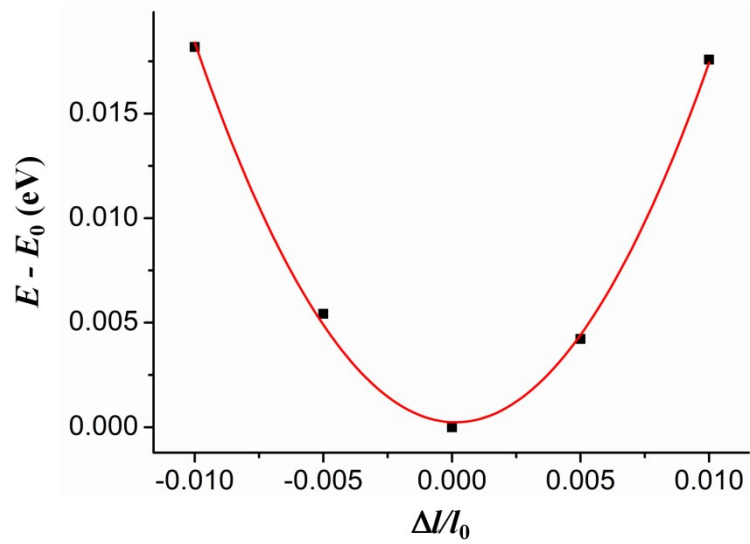
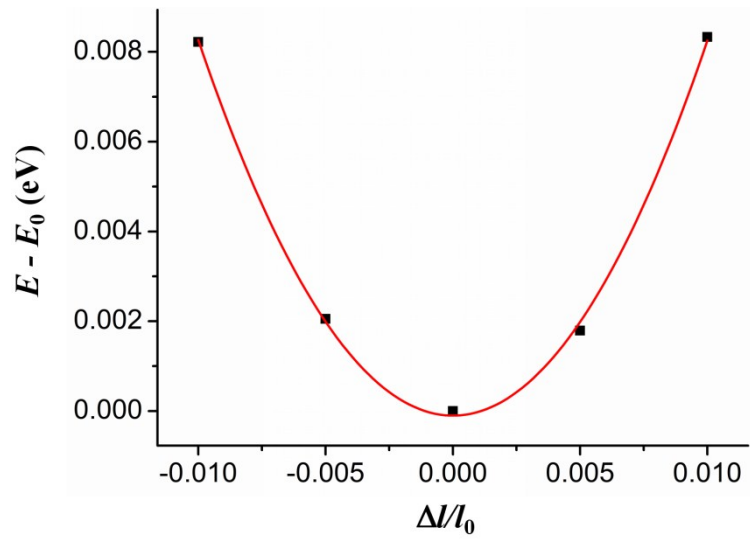


**Fig. S8** Total energy-strain curve of Bi<sub>2</sub>OS<sub>2</sub> mono- and few layers along x/y directions.

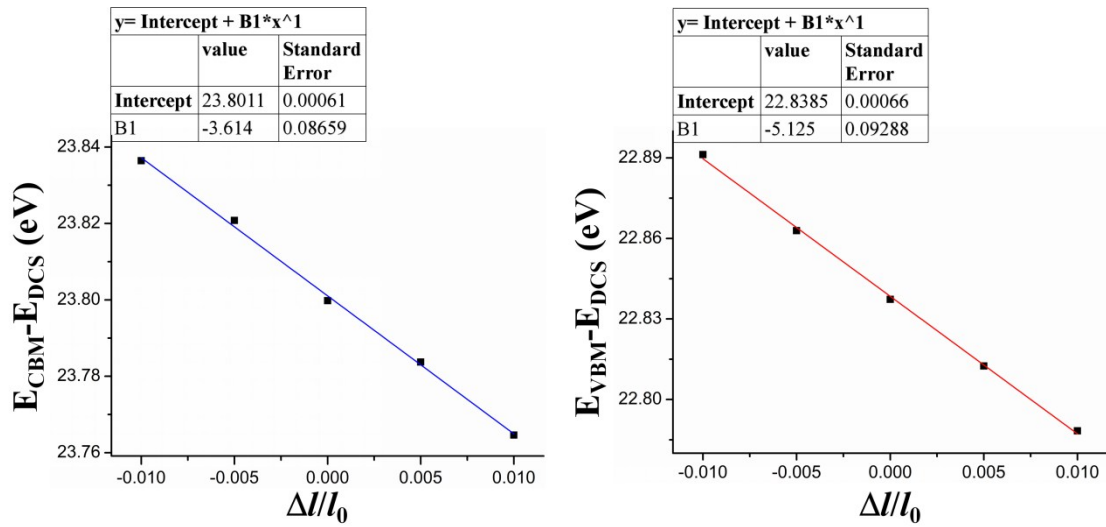


**Fig. S9** Linear fitting of deformation potential. Energy change of the CBM and VBM of  $\text{Bi}_2\text{OS}_2$  bulk with respect to the deep core states (DCS) as a function of lattice dilation.

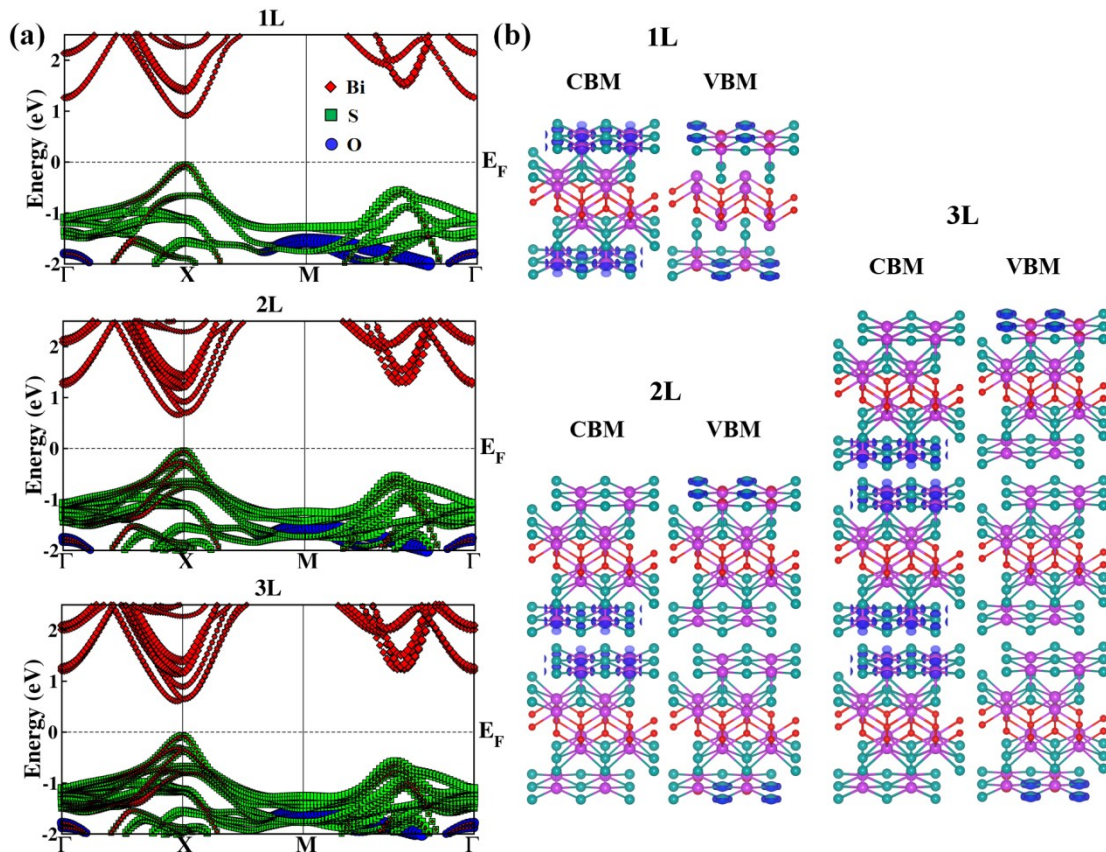


**Fig. S10** (a) Atom-resolved electronic band structures of  $\text{Bi}_2\text{OS}_2$  mono- and few-layers. The red, green, and blue dots represent the contributions from Bi, S, and O atoms. The symbol size is proportional to its population in corresponding atoms. (b)

Partial charge density is indicated in blue for conduction bands near the CBMs with an isovalue of 0.0022 e/bohr<sup>3</sup>, and for valence bands near the VBMs with an isovalue of 0.0003 e/bohr<sup>3</sup>. Magenta, blue-green, and red balls denote Bi, S, and O atoms, respectively.

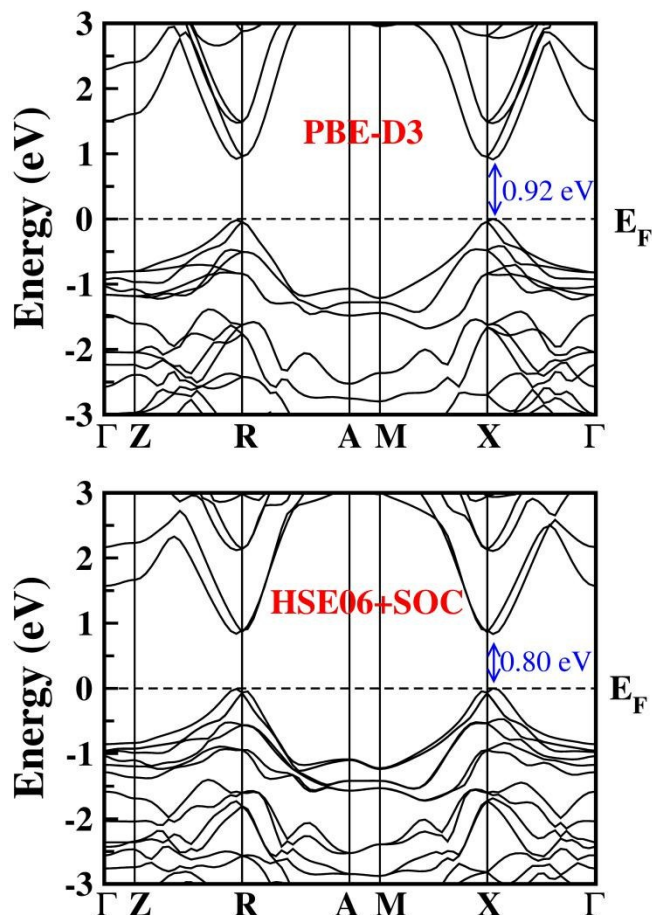


**Fig. S11** Electronic band structures of bulk Bi<sub>2</sub>OS<sub>2</sub> calculated at the PBE-D3 and HSE06+SOC level.

**Table S1** Computed effective mass ( $m^*$ ), 3D elastic modulus ( $C_{3D}$ ), deformation potential constant ( $|E^i|$ ), and in-plane hole and electron mobility ( $\mu$ ) of Bi<sub>2</sub>OS<sub>2</sub> bulk at 300 K

	Carrier Type	$m^*/m_e$	$C_{3D}$ (Gpa)	$ E^i $ (eV)	$\mu$ ( $10^3 \text{ cm}^2\text{V}^{-1}\text{s}^{-1}$ )
<b>Bulk</b>	Electron	0.23	135	3.61	28.8
	Hole	-0.34	135	5.13	4.62